UC Irvine
UC Irvine Previously Published Works

Title

Progress towards high-performance steady-state operation on DIII-D

Permalink

Journal

ISSN

Authors

Greenfield, CM
Murakami, M
Garofalo, AM
et al.

Publication Date

DOI

Copyright Information

Peer reviewed

Progress towards high-performance steady-state operation on DIII-D

C.M. Greenfield [a,*], M. Murakami [b], A.M. Garofalo [c], E.J. Doyle [d], J.R. Ferron [a],
M.R. Wade [a], M.E. Austin [e], S.L. Allen [f], K.H. Burrell [a], T.A. Casper [f], J.C. DeBoo [a],
P. Gohil [a], I.A. Gorelov [a], R.J. Groebner [a], W.W. Heidbrink [g], A.W. Hyatt [a],
G.L. Jackson [a], R.J. Jayakumar [f], K. Kajiwara [a], C.E. Kessel [h], J.E. Kinsey [i], J.Y. Kim [j],
R.J. La Haye [a], L.L. Lao [a], J. Lohr [a], T.C. Luce [a], Y. Luo [g], M.A. Makowski [f],
D. Mazon [k], G.R. McKee [l], M. Okabayashi [h], T.H. Osborne [a], C.C. Petty [a], T.W. Petrie [a],
R.I. Pinsker [a], R. Prater [a], P.A. Politzer [a], H. Reimerdes [c], T.L. Rhodes [d], A.C.C. Sips [m],
J.T. Scoville [a], W.M. Solomon [h], G.M. Staebler [a], H.E. St. John [a], E.J. Strait [a],
T.S. Taylor [a], A.D. Turnbull [a], M.A. Van Zeeland [n], G. Wang [d], W.P. West [a], L. Zeng [d],

the DIII-D Team

[a] *General Atomics, P.O. Box 85608, San Diego, CA 92186-5608, USA*
[b] *Oak Ridge National Laboratory, Oak Ridge, TN, USA*
[c] *Columbia University, New York, NY, USA*
[d] *University of California, Los Angeles, CA, USA*
[e] *University of Texas, Austin, TX, USA*
[f] *Lawrence Livermore National Laboratory, Livermore, CA, USA*
[g] *University of California, Irvine, CA, USA*
[h] *Princeton Plasma Physics Laboratory, Princeton, NJ, USA*
[i] *Lehigh University, Bethlehem, PA, USA*
[j] *Korea Basic Sciences Institute, Daejeon, South Korea*
[k] *Association Euratom-CEA, CEA-Cadarache, St Paul lez Durance, France*
[l] *University of Wisconsin, Madison, WI, USA*
[m] *Institut fur Plasmaphysik, Garching, Germany*
[n] *Oak Ridge Institute for Science and Education, Oak Ridge, TN, USA*

Abstract

Advanced Tokamak research in DIII-D seeks to develop a scientific basis for steady-state high-performance tokamak operation. Fully noninductive ($f_{NI} \approx 100\%$) in-principle steady-state discharges have been maintained for several confinement times. These

* Corresponding author. Tel.: +1 858 455 3686; fax: +1 858 455 4156.
  E-mail address: Chuck.Greenfield@fusion.gat.com (C.M. Greenfield).

plasmas have weak negative central shear with $q_{min} \approx 1.5$–2, $\beta_N \approx 3.5$, and large, well-aligned bootstrap current. The loop voltage is near zero across the entire profile. The remaining current is provided by neutral beam current drive (NBCD) and electron cyclotron current drive (ECCD). Similar plasmas are stationary with $f_{NI} \approx 90$–95% and duration up to 2 s, limited only by hardware. In other experiments, $\beta_N \approx 4$ is maintained for 2 s with internal transport barriers, exceeding previously achieved performance under similar conditions. This is allowed by broadened profiles and active magnetohydrodynamic instability control. Modifications now underway on DIII-D are expected to allow extension of these results to higher performance and longer duration. A new pumped divertor will allow density control in high triangularity double-null divertor configurations, facilitating access to similar in-principle steady-state regimes with $\beta_N > 4$. Additional current drive capabilities, both off-axis ECCD and on-axis fast wave current drive (FWCD), will increase the magnitude, duration, and flexibility of externally driven current.

1. Introduction

There is high confidence that the planned ITER baseline operational scenarios will be capable of achieving fusion gain $Q \approx 10$ in a conventional H-mode regime with edge localized modes (ELMs). This scenario is inherently pulsed, requiring periodic restarts to reset the transformer that drives most of the plasma current. Advanced Tokamak (AT) research at DIII-D [1–3] and elsewhere [4,5] seeks to develop a scientific basis for operational scenarios with similar levels of performance, but capable of operating in steady-state. In addition to all of the requirements for the conventional scenario, AT scenarios require that the transformer driven current be replaced by noninductive current sources.

The most economical current source is the self-generated bootstrap current [6]. We can maximize the bootstrap fraction f_{BS} by operating at high poloidal beta β_p and boundary safety factor q_{95}. However, fusion performance is maximized at high *toroidal* beta β_T and *low* q_{95}. We reconcile these seemingly conflicting requirements by operating at high $\beta_N \propto (\beta_T \beta_p)^{1/2}$, preferably near the ideal-wall pressure limit, and at moderate $q_{95} \approx 4$–5. An additional requirement is that the bootstrap current's spatial distribution, determined by the kinetic profiles, is broad and well-aligned with the desired total current profile.

With a well-designed self-consistent scenario, $f_{BS} = 60$–90% is feasible. The remaining current must be supplied by external sources. In AT experiments in DIII-D, these sources are neutral beam (NBCD), electron cyclotron (ECCD) and fast wave (FWCD) current drive. These experiments have demonstrated in-principle steady-state conditions with noninduc-

tive current fraction $f_{NI} \approx 100\%$, bootstrap fraction $f_{BS} \approx 60\%$, and $\beta_N \approx 3.5$ [7]. Although the pressure profile continues to evolve in these discharges, similar discharges with slightly lower $f_{NI} \approx 90$–95% have been sustained in a stationary condition for the full 2 s pulse length of the gyrotrons which produce the ECCD. These discharges have a slightly reversed safety factor (q) profile with $q_{min} = 1.5$–2.0 and $q_0 - q_{min} \leq 0.5$. The fusion performance in these discharges, as measured by the fusion gain parameter $G = \beta_N H_{89}/q_{95}^2 \approx 0.3$, is at the level expected in the ITER $Q = 5$ steady-state scenario [8].

A second class of discharges has been studied with higher $q_{min} > 2$ and internal transport barriers (ITB) [9]. Using both internal and external coils to null magnetic error fields and actively stabilize resistive wall modes (RWM), these discharges are sustained with $\beta_N \geq 4$ for up to 2 s. Although this scenario has a large f_{NI} approaching unity, these discharges have thus far required plasma current and toroidal magnetic field ramps and so are not yet stationary. The possibilities for bringing this scenario to steady-state conditions are currently under study.

In Section 2, we describe experiments that have obtained fully noninductive conditions in nearly stationary, in-principle steady-state conditions. In Section 3, we discuss discharges at higher β and the conditions necessary to bring them to steady-state. In Section 4, we discuss considerations for our continued development of AT scenarios for ITER and beyond. This includes both our continuing experimental program and an active effort toward integrated modeling, which we anticipate will ultimately produce a predictive capability that applies directly to AT scenario design in future tokamaks.

2. 100% noninductive operation with weak negative shear

Discharges with $q_{min} = 1.5$–2.0, $q_{95} = 4$–5.5 and weak negative central shear ($q_0 - q_{min} \leq 0.5$) form the basis of ITER reference scenario 4 [8], anticipated to obtain steady-state conditions using hardware expected early in ITER operation. In this section, we discuss studies of this scenario in DIII-D (Fig. 1).

The desired target q profile is prepared by triggering an early H-mode, which in turn slows the current penetration resulting in a broad current profile. During the next 2–3 s, β is slowly ramped up using feedback control of the neutral beam, resulting in a highly reproducible target q profile with $q_{min} \approx 2$ and weak negative central shear (Fig. 2). At this time, the neutral beam power is increased to raise β_N to a target value, usually about 3.5, and off-axis ECCD is applied to maintain the current profile in a stationary condition.

During this high-performance phase, both the total and local inductive current approaches zero (Fig. 3). At this time, the plasma current is supplied by bootstrap (59%), NBCD (31%), and ECCD (8%) [7]. The measured [14] noninductive current fraction $f_{NI} = 99.5\%$ is in reasonable agreement with that
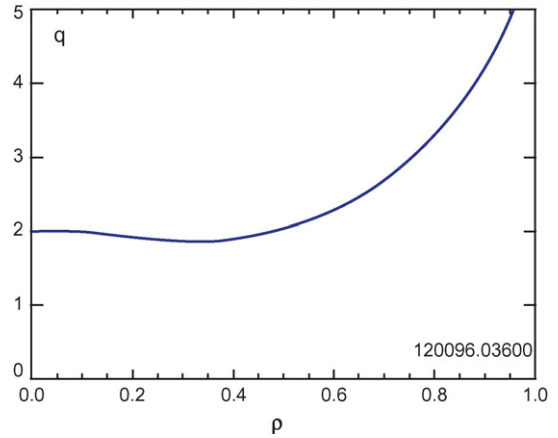

Fig. 2. Target q profile at beginning of high power heating and current drive phase.

calculated by summing the individual contributions. The relatively small contribution from ECCD is very important, as both calculation and previous experience [1] shows that without it, the inductive current would gradually peak near the mid-radius.

Although this discharge is fully noninductive, it is still not stationary. Here, the limitation is due to evolution of the pressure profile rather than the current
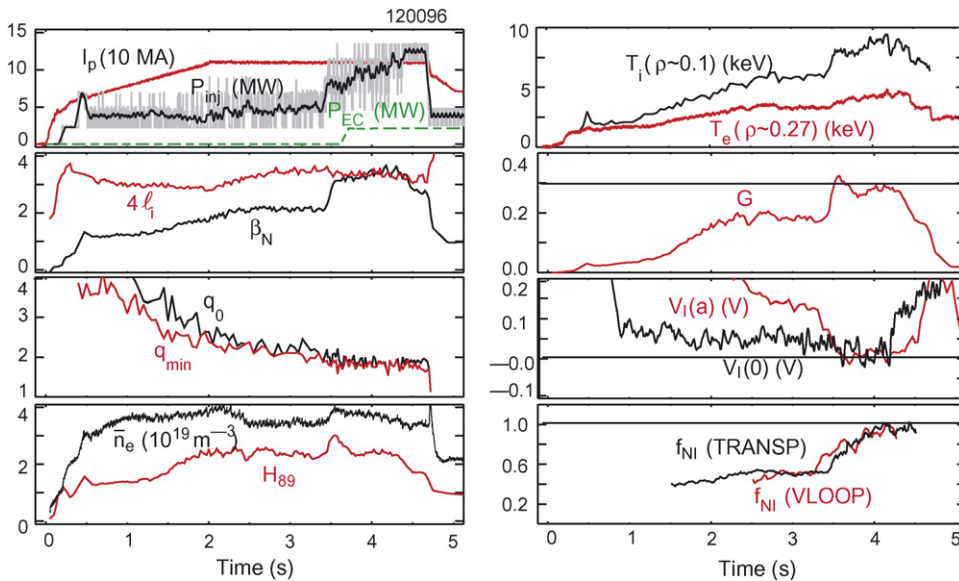

Fig. 1. Waveforms of an AT discharge in DIII-D. Fully noninductive conditions are obtained during the period where $V_1(0) \approx V_1(a) \approx 0$ from 3.6 to 4.2 s. This phase is terminated by an $n = 1$ instability as the pressure profile peakedness increases.
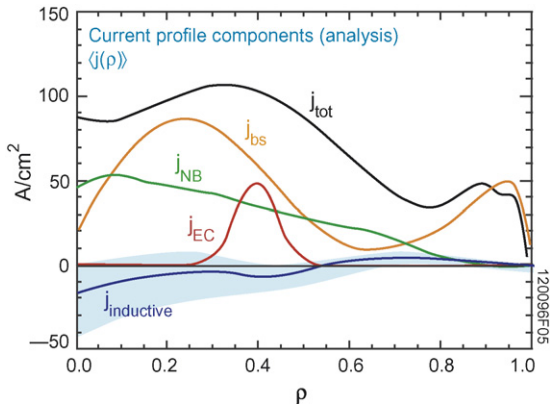
Fig. 3. Components of the current profile during the $f_{NI} \approx 100\%$ phase. The total current profile is calculated by an equilibrium reconstruction [10]. The individual components are calculated by physics-based models: bootstrap current j_{BS} [11] neutral beam driven current j_{NB} [12], and electron cyclotron driven current j_{EC} [13]. The noninductive current is directly calculated from the equilibrium using the method described in Ref. [14].

profile. As β_N gradually increases, the pressure profile becomes more peaked, primarily due to changes in the density profile. As β_N crosses 3.3, the calculated wall position for $n = 1$ marginal stability reaches the DIII-D conformal wall position ($1.45a$) [15]. Soon afterward,

we observe an $n = 1$ fast growing mode that in turn triggers $n = 1$ neoclassical tearing modes.

In similar discharges, a nearly fully noninductive state can be obtained and maintained under stationary conditions for up to 2 s (approximately one current relaxation time), limited by the duration of the gyrotrons that produce the ECCD (Fig. 4). Time histories of the magnetic field pitch angles measured by a motional Stark effect diagnostic (Fig. 4(b)) [16] indicate that current profile evolution stops during this interval, 5–10% of the current is still supplied by inductive means, and the pressure profile remains stationary as well.

As mentioned earlier, it is important to operate AT plasmas at high β_N in order to maximize both fusion gain and bootstrap current. These discharges operate at $\beta_N \approx 3.5$, at or slightly above the no-wall stability limit. Active stabilization of both magnetic error fields and the resistive wall mode [17] is used in these discharges, relying on nonaxisymmetric coils both inside and outside the vacuum vessel. This technique has been successful in allowing routine operation of AT plasmas above the no-wall limit [8]. Future development of this tool is expected to facilitate operation with β_N approaching the ideal wall limit to the $n = 1$ kink mode. Strong plasma shaping has also
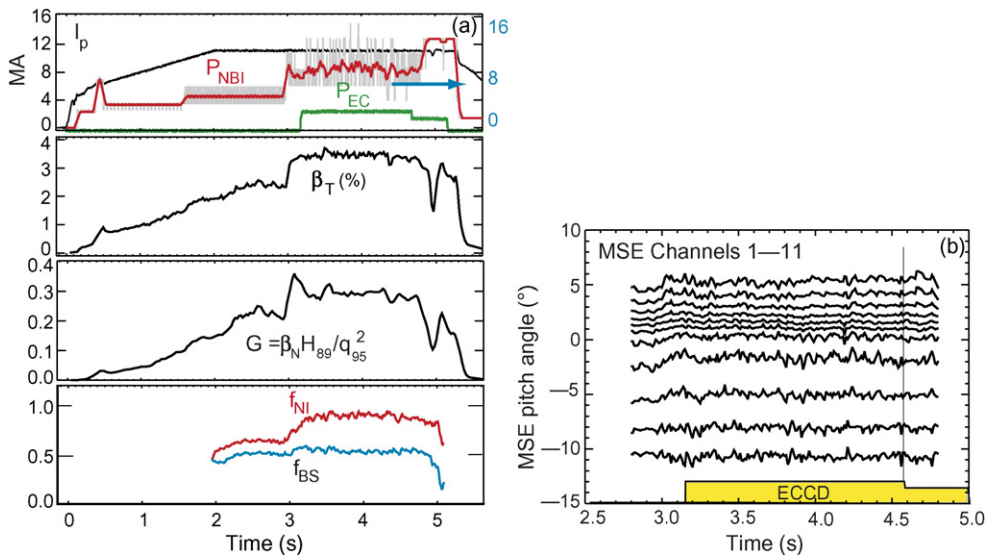

Fig. 4. (a) Time history of a nearly fully noninductive AT discharge with $f_{NI} \approx 90$–95%. This discharge is maintained for the entire duration of the gyrotrons that drive ECCD. (b) The magnetic field line pitch angles measured by MSE are constant during this phase, indicating that the current profile is stationary.

been shown to be beneficial for a high β operation limit [15]. Since ECCD is most efficient at low density and high electron temperatures ($I_{CD} \propto (T_e/n_e)P_{CD}$), the plasma shape used for AT experiments must be matched with the cryopump used to control the density. We are currently adding a second divertor cryopump to allow density control in high triangularity double-null divertor configurations. We anticipate this modification will allow operation with $\beta_N \geq 4$ and $f_{NI} \approx 100\%$ during the upcoming experimental campaign.

We have assembled a database of AT discharges with $f_{NI} = 80$–100%, with durations up to $1\tau_{CR}$. These experiments have achieved normalized fusion performance up to $G = 0.3$ and bootstrap fraction $f_{BS} = 60\%$, consistent with the requirements for the ITER $Q = 5$ steady-state scenario [7].

3. Sustained high β in discharges with an internal transport barrier

We have also obtained high beta discharges in which $\beta_N \approx 4$ is sustained for up to 2 s with $q_{min} > 2$, albeit

under nonstationary conditions [9]. These discharges have low internal inductance ℓ_i, so that $\beta_N > 6\ell_i$, well above the no-wall stability limit, during the high-performance phase. They also have high confinement $H_{89} > 2.5$. The fusion gain factor G uniformly increases throughout the discharge (β_N and H_{89} are nearly constant, but q_{95} is ramping downward with the toroidal magnetic field), eventually exceeding 0.7, well above that needed for the ITER steady-state scenario.

The evolution of one such discharge is shown in Fig. 5. Early neutral beam heating is applied to establish a target with high q_{min}. Off-axis ECCD helps to maintain this state with broad current and pressure profiles. A toroidal magnetic field ramp continues throughout the high-performance phase. Operational experience to date indicates that this ramp is beneficial to maintaining the broad profiles as q_{95} is reduced. The role of the B_T ramp, and whether or not it is necessary, are being evaluated. β_N is maintained at approximately 4 using neutral beam feedback. β_T is not constant, nor is the density.

The magnetic configuration of these discharges are also quite dynamic. The q profile is strongly reversed
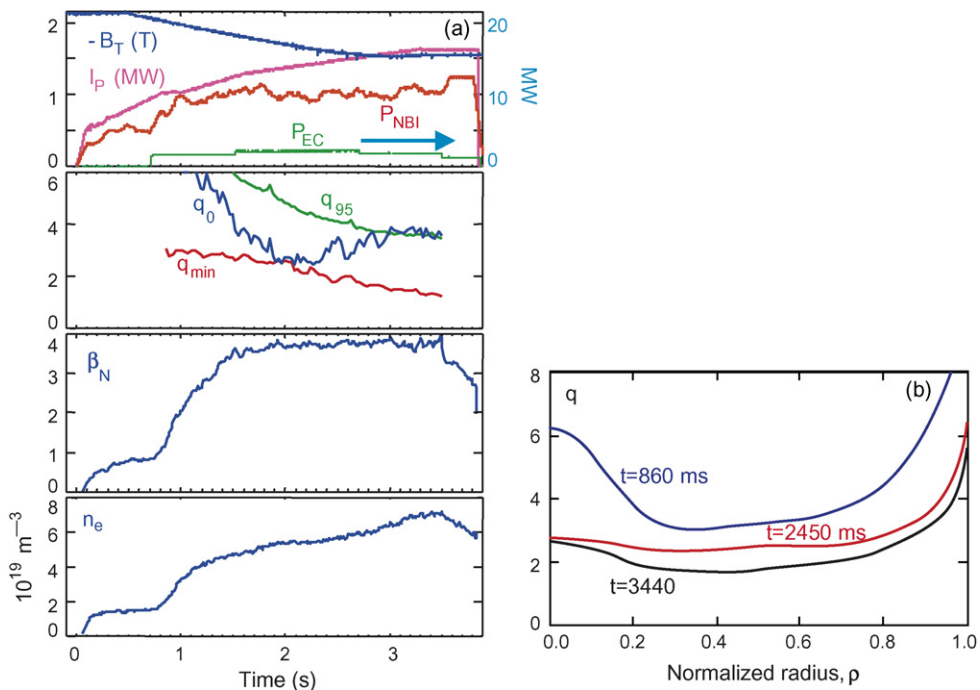

Fig. 5. (a) Time histories of a high β ITB discharge with $\beta_N \approx 4 \approx 6\ell_i$. (b) The q profile evolves slowly throughout the discharge, with $q_{min} > 2$ maintained for much of the high β_N phase.
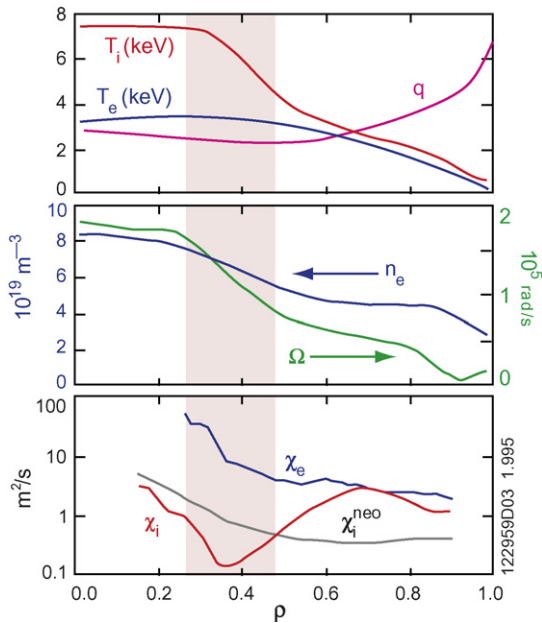
Fig. 6. Profiles during the high β phase indicate the existence of an internal transport barrier in the ion thermal channel. No barrier is evident in the electron channel.

Fig. 7. The calculated ideal-wall β limit for the $n = 1$ kink can be up to $11\ell_i$, far in excess of the no-wall limit. β in this discharge was limited by confinement and the available heating power rather than stability.

at the beginning of the high β phase. In the discharge shown, it becomes flat and then reverses again later in the discharge, all without significant changes in confinement and stability. The minimum safety factor q_{min} continues to evolve, with benign tearing modes appearing and disappearing as q_{min} passes through various rational surfaces. The high performance is usually terminated without disruption by an $(m,n) = (2,1)$ neoclassical tearing mode as q_{min} approaches 1.5.

Examination of the profiles reveals an internal transport barrier forming in the ion thermal channel (Fig. 6). This is evident both in the measured T_i profile and in the ion diffusivity determined by analysis with the TRANSP transport code [12]. Similar to many other such "hot ion" regimes [18], no such barrier appears in the electron thermal or particle transport channels.

The accessibility of high β in these discharges seems unusual in light of several earlier observations. Stability limits usually appear at $\beta_N \leq 3$ in discharges with ITBs [19] due to the associated highly peaked pressure profile. In AT experiments, as described in Section 2, high β is usually difficult to obtain with high $q_{min} > 2$ [15].

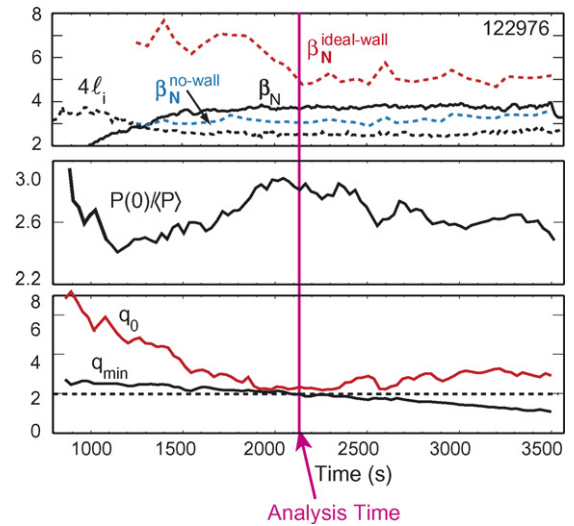Resistive wall mode stabilization is essential to maintaining high β in these discharges. Development

of these discharges included a successful effort to optimize simultaneous feedback control of both internal and external sets of $n = 1$ magnetic coils to dynamically correct error magnetic fields and to exert active control of the RWM. These plasmas are particularly well suited to this correction due to their broad current channel, which couples well to the vessel wall and control coils.

In Fig. 7, the calculated ideal-wall β limit for the $n = 1$ kink mode is shown as calculated by DCON [20], indicating that the stability limit is at $\beta_N \approx 11\ell_i > 5$. Further analysis at the time indicated on the figure (2.05 s) finds that the ideal-wall stability limits to the $n = 1$, 2 and 3 kink modes increase with q_{min} above 2. The no-wall limit does not increase at higher q_{min}, consistent with the previous observations [15]. These stability calculations indicate that considerable increases in β may still be available in these discharges if RWM control is maintained.

The potential for these discharges as a steady-state candidate are presently under evaluation. They do have a high noninductive fraction, although interpretation of the exact fraction has been difficult due to their nonstationary nature. It is thought that the role of the toroidal field ramp may be to broaden the current profile by adding a small current at large radius. We may

be able to replace this current with ECCD as more microwave power becomes available. Even if a tool not available on DIII-D is required to drive current sufficiently far off-axis, this regime may still prove useful for future devices with the inclusion of such a current drive source.

4. Considerations for future at development

In the previous two sections, we have shown two demonstrations of experimental progress toward our goal of steady-state high performance. The most important product of this research, however, is anticipated to be a predictive capability that can be used to design such scenarios for future devices such as ITER. Our approach couples experimental and integrated modeling efforts; theory-based modeling is used both to design experiments and to interpret their results. For example, the results shown in Section 2 were a direct result of such modeling activities applied to previous discharges [21]. The results are fed back to the model development, resulting in a coupled evolution of both the experimental efforts and the models themselves.

Fig. 8 shows such a simulation of the current profile components in a $f_{NI} = 100\%$ discharge using DIII-D capabilities expected for upcoming experiments [7].
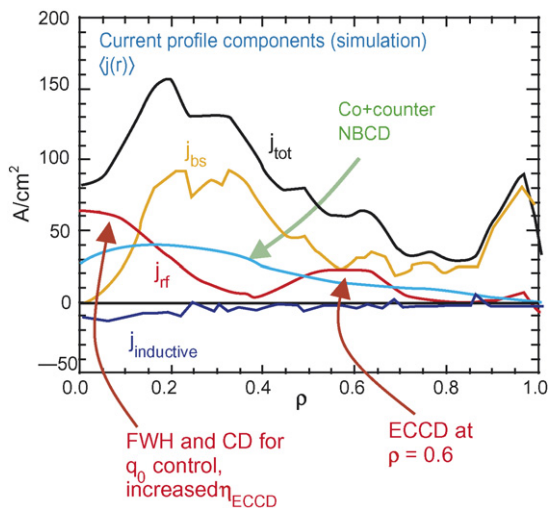

Fig. 8. Theory-based integrated modeling predicts improved performance in future DIII-D AT experiments utilizing hardware upgrades now in progress. $P_{EC} = 4.5\,MW$, $P_{NB} = 6.8\,MW$, $P_{FW} = 3.5\,MW$, $I_p = 1.19\,MA$, $B_T = 1.86\,T$, $\beta_T = 4.1\%$, $\beta_N = 3.8$.

Theory-based models are used to calculate the sources and core transport [3], with the pedestal parameters calculated empirically. This approach successfully reproduces most of the features of the present discharges, and gives promising results for performance with modifications to DIII-D now underway. The same approach has been applied to ITER, assuming "day 1" capabilities, and indicates steady-state performance with $Q = 5$ [8] is possible.

Future AT development will also be facilitated by several hardware improvements now underway in DIII-D [21]. The aforementioned scenario modeling makes use of some of these. As previously mentioned, the highest performance is obtained with strongly shaped double-null geometry. Effective current drive, however, requires operation with limited density, which has not been possible in DIII-D since only the upper divertor couples to a cryopump in this geometry. A new high triangularity lower divertor cryopump is being installed in DIII-D, which is expected to allow stable operation of double-null AT plasmas with $\beta_N > 4$.

The discharges discussed in the present work were done with rather limited ECCD power, which has only been available for 2 s pulse lengths. The gyrotron system that generates the ECCD is currently being upgraded to include six 1 MW long-pulse gyrotrons. The upgraded system will be capable of delivering approximately 4.5 MW of power to the plasma, maintained for up to 10 s.

Fast wave heating (FWEH) and current drive (FWCD) has not been available on DIII-D for several years; these systems are also being restored. Although their capability for driving current in strongly beam-heated plasmas in not established, we expect this system to at least be capable of heating electrons and thereby improving the efficiency of ECCD.

The final major modification being made to DIII-D is the rotation of one neutral beamline, containing two (out of a total of eight) neutral beams to allow mixed co- and counter-NBI. This will allow some control (although not independent) of both NBCD and plasma rotation at constant heating power.

5. Summary

Advanced Tokamak research in DIII-D seeks to establish a scientific basis for high-performance

steady-state operation in a future tokamak reactor. In this paper, we describe experimental studies of two scenarios that demonstrate many desirable features as we move toward this goal.

Fully noninductive operation of discharges with weak negative magnetic shear in the core has been achieved, with $\beta_N \approx 3.5$, $q_{min} = 1.5$–2.0 and $q_0 - q_{min} = 0$–0.5. These discharges demonstrate the performance needed for the ITER $Q = 5$ steady-state scenario. Although the current profile evolution stops in discharges with $f_{NI} \approx 100\%$, the pressure profile continues to evolve. An important component of future research will be development of improved control over such plasmas toward allowing a completely steady-state condition. Better control has been established in similar plasmas with a small amount (5–10%) of inductive current. Such discharges have been maintained in a stationary condition for up to $1\tau_R$, limited only by hardware considerations.

In a second set of experiments, discharges with internal transport barriers and high safety factor have maintained $\beta_N \approx 6\ell_i \approx 4$ for up to 2 s, significantly above the no-wall limit to kink modes. These high levels of β, facilitated by simultaneous active control of magnetic error fields and the resistive wall mode, are still well below the ideal-wall stability limit, calculated at up to $\beta_N \approx 11\ell_i$. Although these discharges have a large amount of noninductive current, they are not stationary due to the requirement of a toroidal field ramp throughout the high-performance phase. Future work in this regime will include a more accurate assessment of the role of this ramp, and the means to replace it in a fashion that allows steady-state operation.

DIII-D is currently undergoing several modifications to improve our capabilities to carry out AT research. A high triangularity divertor cryopump is being added to the bottom of the DIII-D vessel, mirroring one on the top, to allow density control in a double-null configuration. This is expected to allow operation of weak negative shear AT plasmas with $\beta_N > 4$ and density control to allow efficient current drive. Our current drive capabilities will be enhanced by the availability of about 4.5 MW (absorbed) of ECCD power with 10 s pulse lengths, sufficient to maintain the discharge for several current relaxation times. DIII-D FW capabilities are also being restored, providing the ability to increase the electron temperature for improved ECCD efficiency, and possible direct control of the on-axis

plasma current. Conversion of two (out of eight) neutral beam sources to counter-injection will give additional (simultaneous) control of core rotation and current.

A theory-based integrated modeling effort is strongly coupled with the experimental program. Simulations are used to both design and interpret the experiments. Results of these studies feed back into the model development itself, so that the accuracy of the modeling continually improves along with our experimental capabilities. These simulations reproduce present experiments quite well, and promise further progress utilizing the new hardware now becoming available. The same modeling tools predict the ITER $Q = 5$ steady-state scenario can be successful using "day 1" heating and current drive tools.

Acknowledgments

References

[1] M.R. Wade, T.C. Luce, P.A. Politzer, J.R. Ferron, S.L. Allen, M.E. Austin, et al., Progress toward long-pulse high-performance advanced tokamak discharges on the DIII-D tokamak, Phys. Plasmas 8 (2001) 2208–2216.

[2] C.M. Greenfield, M. Murakami, J.R. Ferron, M.R. Wade, T.C. Luce, C.C. Petty, et al., High performance advanced tokamak regimes in DIII-D for next-step experiments, Phys. Plasmas 11 (2004) 2616–2626.

[3] M. Murakami, C.M. Greenfield, M.R. Wade, T.C. Luce, J.R. Ferron, H.E. St. John, et al., 100% noninductive operation at high beta using off-axis ECCD in DIII-D, Nucl. Fusion 45 (2005) 1419–1426.

[4] X. Litaudon, A. Bécoulet, F. Crisanti, R.C. Wolf, Yu.F. Baranov, E. Barbato, et al., Progress towards steady-state operation and real-time control of internal transport barriers in JET, Nucl. Fusion 43 (2003) 565–572.

[5] S. Ishida, JT-60 Team and JFT-2M Group, High-beta steady-state research and future directions on the Japan Atomic Energy Research Institute Tokamak-60 upgrade and the Japan Atomic

Energy Research Institute Fusion Torus-2 modified, Phys. Plasmas 11 (2004) 2532–2542.

[6] R.J. Bickerton, J.W. Connor, J.B. Taylor, Diffusion driven plasma currents and Bootstrap tokamak, Nat. Phys. Sci. 229 (1971) 110–112.

[7] M. Murakami, M.R. Wade, C.M. Greenfield, T.C. Luce, J.R. Ferron, H.E. St. John, et al., Progress toward fully noninductive, high beta conditions in DIII-D, Phys. Plasmas 13, 056106 (2006).

[8] W.A. Houlberg, C. Gormezano, J.F. Artaud, E. Barbato, V. Basiuk, A. Becoulet, et al., Integrated modeling of the current profile in steady-state and hybrid ITER scenarios, Nucl. Fusion 45 (2005) 1309–1320.

[9] A.M. Garofalo, E.J. Doyle, J.R. Ferron, C.M. Greenfield, R.J. Groebner, A.W. Hyatt, et al., Access to sustained high-beta with internal transport barrier and negative central shear in DIII-D, Phys. Plasmas 13, 056110 (2006).

[10] L.L. Lao, J.R. Ferron, R.J. Groebner, W. Howl, H. St. John, E.J. Strait, T.S. Taylor, Equilibrium analysis of current profiles in tokamaks, Nucl. Fusion 30 (1990) 1035–1049.

[11] O. Sauter, C. Angioni, Y.R. Lin-Liu, Neoclassical simulations of fusion alpha particles in pellet charge exchange experiments on the tokamak fusion test reactor, Phys. Plasmas 6 (1999) 2834–2839.

[12] R.J. Hawryluk, An empirical approach to tokamak transport, in: B. Coppi, et al. (Eds.), Physics Close to Thermonuclear Conditions, vol. 1, Commission of the European Communities, Brussels, 1980, pp. 19–46.

[13] Y.R. Lin-Liu, V.S. Chan, R. Prater, Electron cyclotron current drive efficiency in general tokamak geometry, Phys. Plasmas 10 (2003) 4064–4071.

[14] C.B. Forest, K. Kupfer, T.C. Luce, P.A. Politzer, L.L. Lao, M.R. Wade, et al., Determination of the noninductive current profile in tokamak plasmas, Phys. Rev. Lett. 73 (1994) 2444–2447.

[15] J.R. Ferron, T.A. Casper, E.J. Doyle, A.M. Garofalo, P. Gohil, C.M. Greenfield, et al., Optimization of DIII-D Advanced Tokamak discharges with respect to the β limit, Phys. Plasmas 12 (2004) 056126-1–056126-10.

[16] B.W. Rice, K.H. Burrell, L.L. Lao, Y.R. Lin-Liu, Direct measurement of the radial electric field in tokamak plasmas using the stark effect, Phys. Rev. Lett. 79 (1997) 2694–2697.

[17] A.M. Garofalo, R.J. La Haye, J.T. Scoville, Analysis and correction of intrinsic non-axisymmetric magnetic fields in high-β DIII-D plasmas, Nucl. Fusion 42 (2002) 1335–1339.

[18] C.M. Greenfield, D.P. Schissel, B.W. Stallard, E.A. Lazarus, G.A. Navratil, K.H. Burrell, et al., Transport and performance in DIII-D discharges with weak or negative central magnetic shear, Phys. Plasmas 4 (1997) 1596–1604.

[19] E.J. Doyle, C.M. Greenfield, M.E. Austin, L.R. Baylor, K.H. Burrell, T.A. Casper, et al., Progress towards increased understanding and control of internal transport barriers in DIII-D, Nucl. Fusion 42 (2002) 333–339.

[20] A.H. Glasser, M.S. Chance, Determination of free boundary ideal MHD stability with DCON and VACUUM, Bull. Am. Phys. Soc. 42 (1997) 1848.

[21] C.M. Greenfield, M. Murakami, J.R. Ferron, M.R. Wade, T.C. Luce, C.C. Petty, et al., Advanced Tokamak research in DIII-D, Plasma Phys. Control. Fusion 46 (2004) B213–B233.